Separation Science and Technology
Publication details, including instructions for authors and subscription information:
http://www.informaworld.com/smpp/title~content=t713708471

Analysis of Feed Effects on a Single-Stage Gas Centrifuge Cascade

Houston G. Wood[a]
[a] DEPARTMENT OF MECHANICAL, AEROSPACE & NUCLEAR ENGINEERING UNIVERSITY OF VIRGINIA, CHARLOTTESVILLE, VIRGINIA

To cite this Article Wood, Houston G.(1995) 'Analysis of Feed Effects on a Single-Stage Gas Centrifuge Cascade', Separation Science and Technology, 30: 13, 2631 — 2657
To link to this Article: DOI: 10.1080/01496399508013707
URL: http://dx.doi.org/10.1080/01496399508013707

SEPARATION SCIENCE AND TECHNOLOGY, 30(13), pp. 2631–2657, 1995

Analysis of Feed Effects on a Single-Stage Gas Centrifuge Cascade

HOUSTON G. WOOD III
DEPARTMENT OF MECHANICAL, AEROSPACE & NUCLEAR ENGINEERING
UNIVERSITY OF VIRGINIA
CHARLOTTESVILLE, VIRGINIA 22903

ABSTRACT

The Onsager pancake model for the fluid dynamics of the countercurrent flow of gas in a centrifuge is used to study the separation performance of a single-stage gas centrifuge cascade. Based on the fluid dynamic solutions, Cohen–Onsager theory is used to calculate the separative performance. The separation considered is the enrichment of natural ^{235}U to 3%. The effects of the introduction of the feed gas on the separation performance are studied, and this work is compared to similar work by Rätz who used a much simpler model. The present work agrees well with the simpler model on predictions of separative performance but not on parameters such as the axial location of the feed stream.

1. INTRODUCTION

Over the past years, most of the interest in gas centrifuges has been for the enrichment of uranium in the fissionable isotope ^{235}U. However, with the current abundant supply of enriched uranium, interest has been growing in using gas centrifuges to separate stable isotopes. The papers by Roberts (1) and Szady (2) have described some of the efforts to separate stable isotopes in the United States. Recent papers by Ying et al. (3), Borisevich et al. (4), and Fillippov et al. (5), presented at the Fourth Workshop on Separation Phenomena in Liquids and Gases held in Beijing, describe activities to separate stable isotopes by gas centrifuges in China and Russia. With modern gas centrifuges it is often possible to attain the desired separation in a single machine whether it be uranium or other isotopes. In this paper we consider a gas centrifuge for enriching uranium to study the effects of feed flow on the separation in a single-stage gas centrifuge cascade. A similar analysis can be applied to other isotopic mixtures.

The fissionable isotope ^{235}U occurs naturally at a concentration of 0.711% by weight, and nuclear power reactors require a fuel of approximately 3.0% ^{235}U. Some of the schemes for producing this enriched product rely on connecting separating elements in a cascade. In particular, gas centrifuges are generally connected in series to provide the necessary enrichment and in parallel to provide the necessary throughput. However, centrifuges can be designed to produce a product of 3% ^{235}U in a single machine. Rätz (6) analyzed this problem and varied such parameters as length, diameter, operating speed, and feed rate. Because of approximations in the fluid dynamic model used by Rätz, it allows the easy calculation of numerous conditions. However, it seems reasonable to use a less approximate model to check the trends predicted by the simpler model.

In this study we have used the Onsager pancake model with sources and sinks of mass, momentum, and energy which has been described by Wood and Morton (7), Wood and Sanders (8), and Wood and Babarsky (9). The introduction of the feed gas plays an important role in establishing the secondary countercurrent flow which produces the axial separation gradient. Rätz's model does not account for this feed effect. In this study attention has been given to modeling the feed introduction and to using the model to study the effect on the separation.

For a fixed length, diameter, and wall pressure, the separative work is calculated as a function of feed rate for several operating speeds. The pancake model and Rätz's model predict very similar results for the feed rate that gives 3% enrichment. However, the models predict very different results for the optimal axial position for the feed introduction. These results are analyzed as well as the details of the fluid dynamic solutions.

2. FLUID DYNAMICS MODEL

The fluid dynamics model used in this study is the Onsager pancake equation with the inclusion of internal source/sink terms. The derivation of the equations has been reported in numerous places (7–9). In this model the solution to the equations of motion for a viscous heat-conducting compressible ideal fluid is assumed to be representable as a perturbation about solid body isothermal flow in a right circular cylinder. The perturbation equations can be combined into a single sixth-order, linear partial differential equation

$$(e^x(e^x\chi_{xx})_{xx})_{xx} + B^2\chi_{yy} = F(x, y) \tag{2.1}$$

where χ is a master potential from which the physical variables can be extracted. The independent variable

$$x = A^2\left[1 - \left(\frac{r}{a}\right)^2\right]$$

is the radial scale height or e-folding distance for the density and y is the axial variable scaled by the radius, a, of the cylinder. The variable $B^2 = \mathrm{Re}^2 S/16A^{12}$ is a parameter containing the physical description of the particular rotor and operating parameters. In particular $\mathrm{Re} = \rho_w \Omega a^2/\mu$ where ρ_w is the density at the wall, Ω is the frequency of rotation, and μ is the viscosity where the bulk viscosity has been taken to be 0. The quantity $S = 1 + \mathrm{Pr}A^2(\gamma - 1)/2\gamma$ is a thermodynamic variable where γ is the ratio of specific heats and Pr is the Prandtl number. The speed parameter is $A^2 = \Omega^2 a^2/2RT_0$, where T_0 is the average temperature of the gas and R is the specific gas constant. The nonhomogeneous term $F(x, y)$ arises from internal sources or sinks of mass, momentum, or energy, and is written

$$\begin{aligned} F(x, y) = {} & \frac{B^2 A^2}{2\mathrm{Re}S} \int_x^{x_T} (Z_y - 2V_y)\, dx' \\ & - \frac{B^2}{2\mathrm{Re}S} \int_x^{x_T} \int_0^{x'} (Z_y + 2(S - 1)V_y)\, dx' dx'' \\ & - \frac{B^2}{4A^4} \int_x^{x_T} \int_0^{x'} M_y dx' dx'' \\ & - \frac{B^2 A^2}{2\mathrm{Re}S} [(e^x U_y)_x + (e^x W)_{xx}] \end{aligned} \quad (2.2)$$

Here M, U, V, W, and Z are dimensionless quantities which represent source terms in the modified forms of the conservation equations for mass, momentum, and energy. In terms of the dimensional physical variables, the source of mass is M, the source of momentum is $\mathbf{F}_s = (F_r, F_\theta, F_z)$, and sources of heat and work are Q and W. The mass introduced by the source has temperature T_s, velocity $\mathbf{V}_s = (V_r, V_\theta, V_z)$, and the local velocity of the rotating gas is assumed to be given by solid body rotation or $\mathbf{q} = (0, \Omega r, 0)$. The quantities in Eq. (2.2) are related to these physical variables as follows:

$$M = \mathrm{M}/\rho_w \Omega \quad (2.3a)$$

$$U = (\mathrm{M}v_r + F_r)/\rho_w \Omega^2 a \quad (2.3b)$$

$$V = (\mathrm{Re}/4A^4)\,[(v_\theta - \Omega r)\mathrm{M} + F_\theta]/\rho_w\Omega^2 a \tag{2.3c}$$

$$W = 2A^2[\mathrm{M}v_z + F_z]/\rho_w\Omega^2 a \tag{2.3d}$$

$$Z = \frac{1}{4A^4}\left\{Q + W - q\cdot F_s + M\left[\frac{(V_s - q)^2}{2} - c_p(T_0 - T_s)\right]\right\}\Big/(kT_0/a^2) \tag{2.3e}$$

3. A FEED MODEL

At high rates of rotation, the gas is compressed into a narrow annular region near the cylinder wall and a very good vacuum is established in the center region of the centrifuge. The feed gas is introduced from a hole in the pipe which is located along the axis of rotation (see Fig. 1). We assume the stagnation conditions in the feed reservoir are known, and that the hole is a choked orifice. This allows the velocity and temperature of the expanded gas to be determined. Further, this expanded gas is frozen in all of its modes except the translational mode. Therefore, the gas continues with this temperature along the trajectory until it reaches the denser region and collides with the rotating gas. We assume that this collision occurs at a radial position where the mean free path is equal to a local density scale height, and that with one collision the feed gas is accelerated to rotational speed. We assume the expansion from stagnation conditions T_0, $V_0 \simeq 0$ to T_s, V_s is adiabatic so that $c_p(T_0 - T_s) = \frac{1}{2}V_s^2$ which is substituted into Eq. (2.3e). Therefore the source terms which model the introduction of feed are

$$M = \mathrm{M}/\rho_w\Omega \tag{3.1a}$$

$$U = \mathrm{M}v_r/\rho_w\Omega^2 a \tag{3.1b}$$

$$V = (\mathrm{Re}/4A^4)\,(v_\theta - \Omega r)\mathrm{M}/\rho_w\Omega^2 a \tag{3.1c}$$

$$W = 2A^2\mathrm{M}v_z/\rho_w\Omega^2 a \tag{3.1d}$$

$$Z = (a/4A^4)\mathrm{M}^{1/2}[(V_s - q)^2 - V_s^2]/(kT_0/a^2) \tag{3.1e}$$

The conditions of no shear and no heat flux are imposed on Eq. (2.1) at the inner boundary or top of the atmosphere at a radial location $x = x_T$, where x_T is chosen large enough so that the solution is independent of the choice. Numerical experiments have shown that $x_T = 15$ is large enough, and this value is generally used. This is consistent with the analysis of this problem by Cooper and Morton (10). The radial location of the feed gas collision depends on operating parameters such as the rotation rate and inventory, and for the cases considered range from approximately

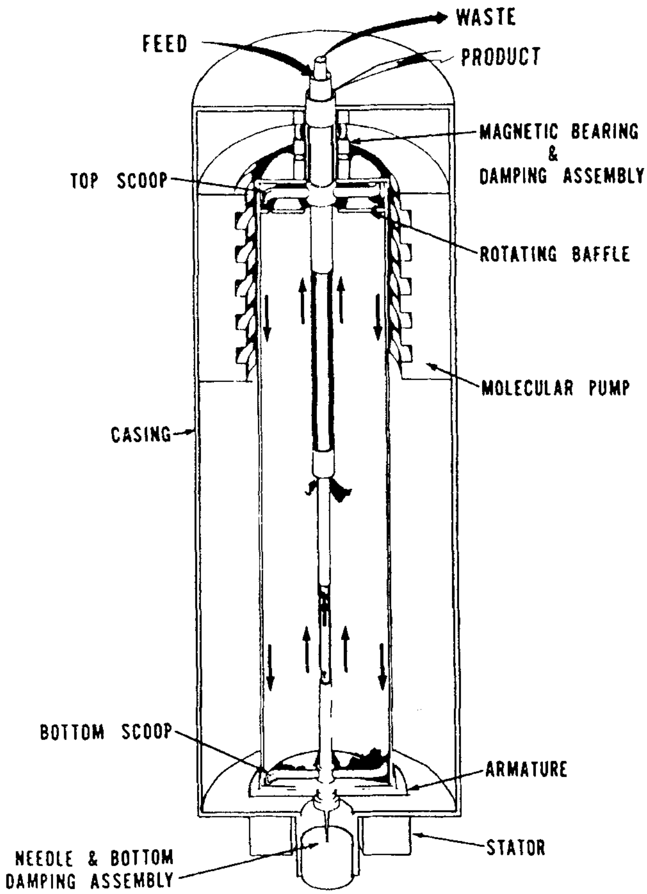

FIG. 1 Early model gas centrifuge.

$x = 8$ to $x = 10$. Because of the assumptions regarding the feed, the boundary conditions at $x = x_T$ are *not* changed.

The mass that is introduced by the feed can be removed through a boundary or a sink. Again referring to Fig. 1 with an upper baffle, a model of this geometric configuration would allow for mass removal through the upper boundary and through a sink located at the position corresponding to the bottom scoop. This scoop is stationary and acts as a sink of angular momentum or a source of drag. Therefore, $\mathbf{F}_s = (0, F_\theta, 0)$, where F_θ is the drag force exerted by the scoop, and $\mathbf{q}\cdot\mathbf{F}_s = \Omega r^* F_0$ is the scoop drag power. The source model for the scoop drag is then

$$M = U = W = 0 \tag{3.2a}$$

$$V = (\mathrm{Re}/4A^4)F_\theta/\rho_w\Omega^2 a \tag{3.2b}$$

$$Z = -(1/4A^4)\Omega r^* F_\theta/(kT_0/a^2) \tag{3.2c}$$

Here, F_θ is negative since the scoop is a sink of angular momentum. If the valve is closed so that no mass is removed by the scoop, Eq. (3.2) models the action of the scoop on the gas. If mass is removed by the scoop, the source terms will be the sum of those given by Eqs. (3.1) and (3.2), with M taken as negative to reflect a sink of mass.

If the control volume used is taken in front of the scoop, the gas can be assumed to leave the system with velocity of solid body rotation so that $\mathbf{V}_s = (0, \Omega r^*, 0)$. For example, we see that Eq. (3.1e) is simply

$$Z = -(1/4A^4)\mathrm{M}^{1/2}(\Omega r^*)^2/(kT_0/a^2) \tag{3.3}$$

which represents the kinetic energy of the gas leaving the system.

4. NUMERICAL RESULTS

The centrifuge parameters used in the calculations were chosen from those suggested at the 3rd Workshop on Gases in Strong Rotation held in Rome in 1979. In particular, these are the parameters used by Rätz in his paper presented at the 6th Workshop in Tokyo in 1985. These parameters are given in Table 1.

Several fluid dynamic solutions were calculated and linearly combined to find the optimum separative performance. Figure 2a depicts the streamlines for the countercurrent flow induced by a linear temperature profile along the outer wall of the rotor with constant temperature along the top and bottom horizontal boundaries. The end-to-end temperature difference ΔT is 1 K. Figure 2b is a plot of the flow profile efficiency, e_F, and the separation parameter m as a function of the axial position. [See Hoglund

TABLE 1
Centrifuge Parameters

Length	15 m
Diameter	0.5 m
Wall pressure	500 torr
Peripheral speed	800 m/s
Average gas temperature	315 K

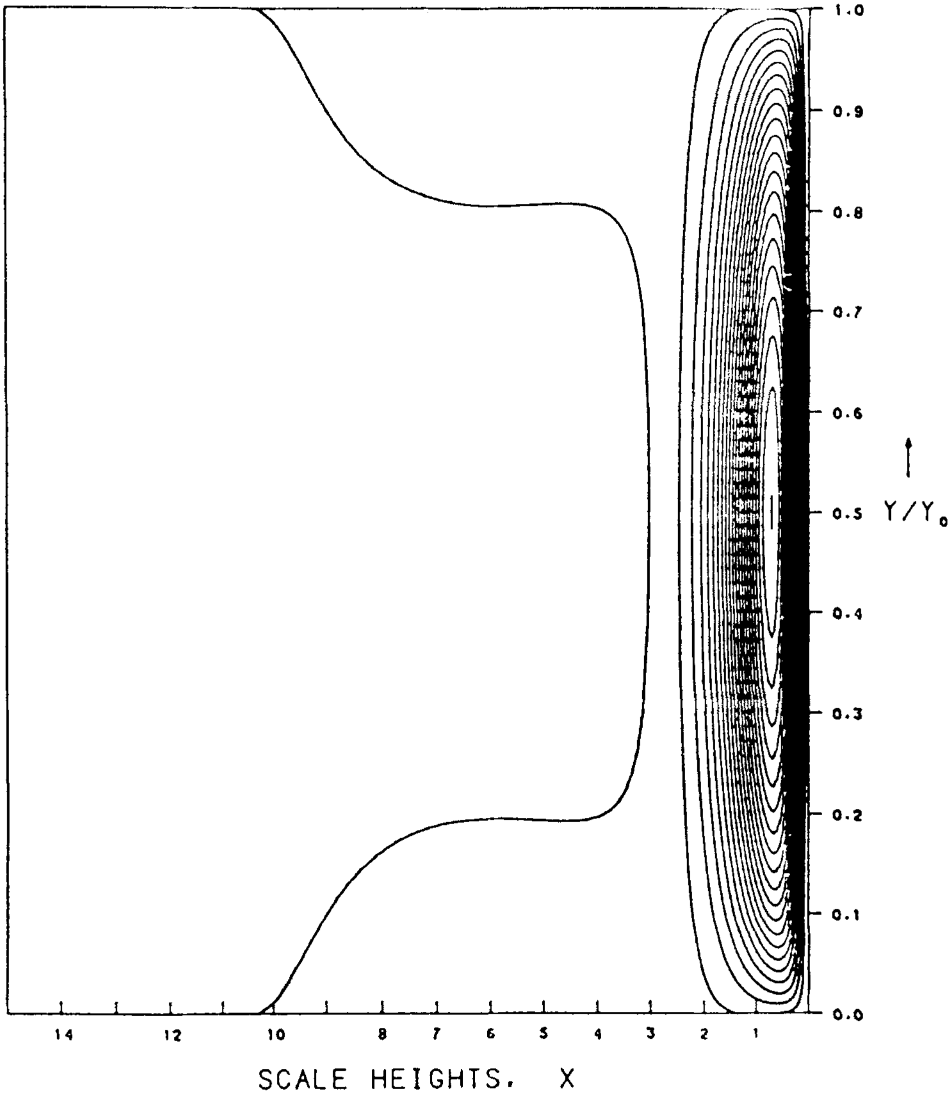

FIG. 2a Streamlines for the wall thermal drive.

et al. (11) for definitions of these parameters.] Figure 3a depicts the streamlines for the countercurrent flow induced by a scoop located at $x = 6.0$, $y = 0.25$. In this calculation the scoop removes no mass and is simulated as a sink of angular momentum of 1000 dynes as described in Eq. (3.2). Figure 3b shows the plots of e_F and m for the scoop case.

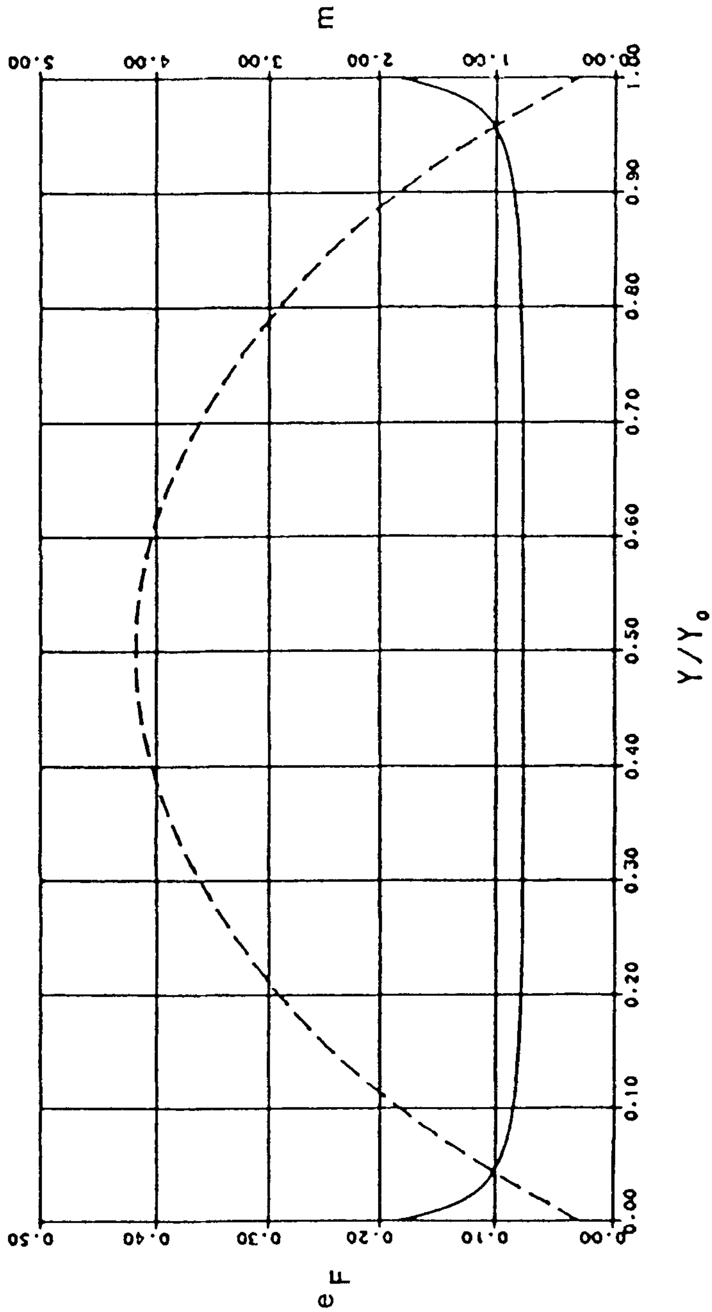

FIG. 2b Separation parameters e_F (——) and m (- -) versus axial position for wall thermal drive with ΔT = 1 K.

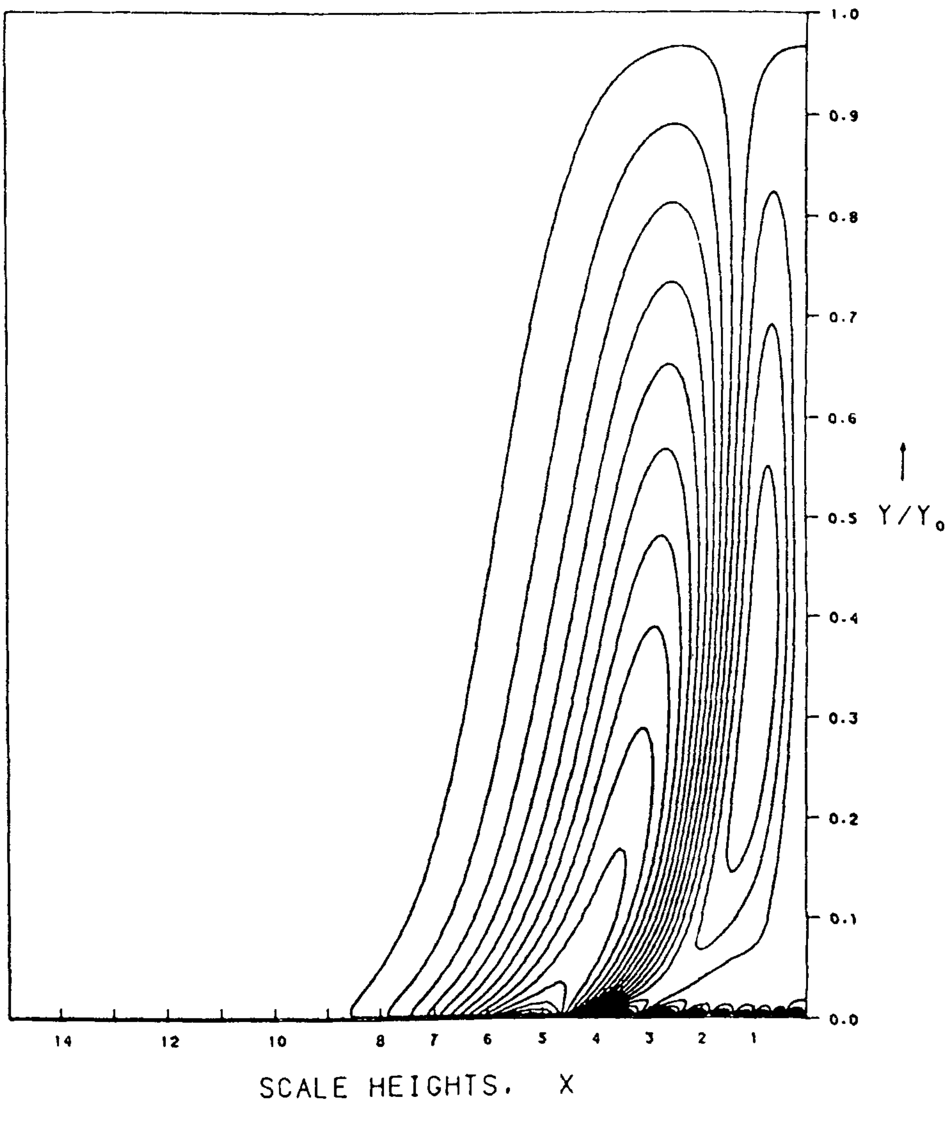

FIG. 3a Streamlines for scoop drive with scoop located at $x = 6.0$, $y = 0.25$.

The next three sets of figures are for calculations using three different ways of introducing the feed. In all three cases, a feed of 1 kg/s is introduced at the axial midplane and removed through ports in the top and bottom boundaries located between $x = 5.5$ and $x = 6.5$. The cut, or

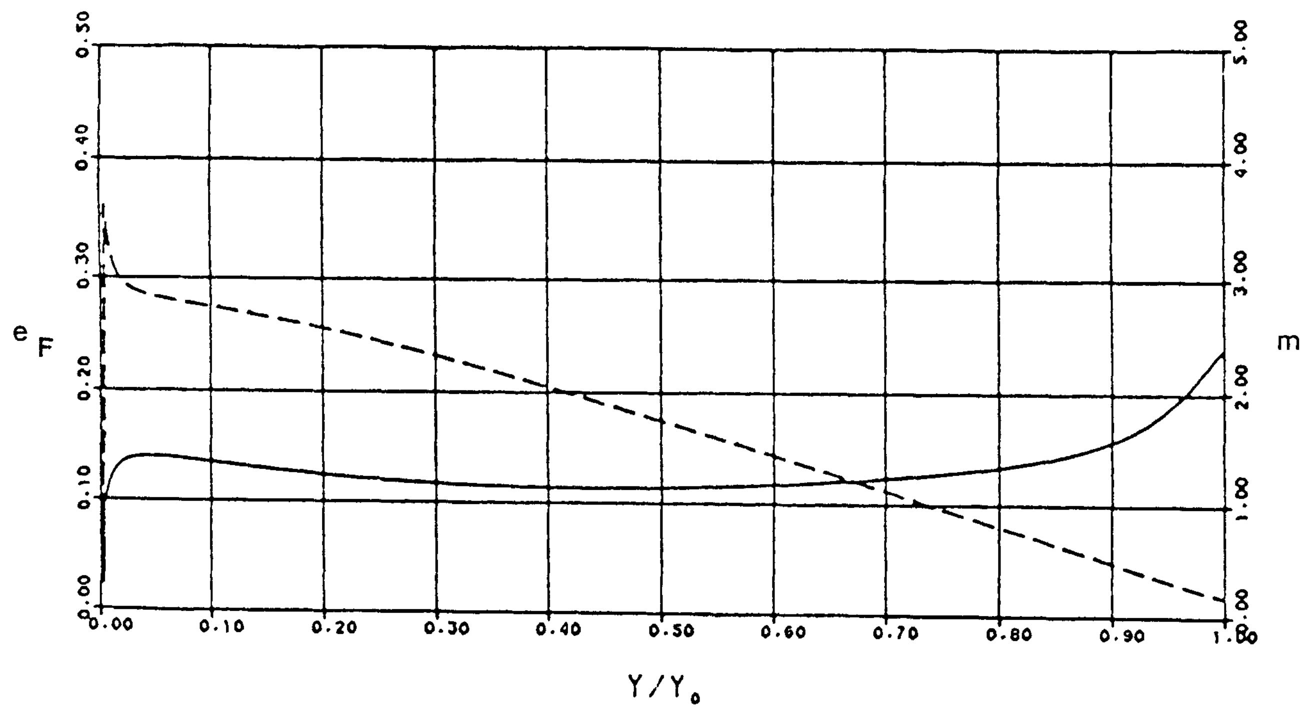

FIG. 3b Separation parameters e_F (——) and m (- -) versus axial position for scoop drive with a drag of 1000 dynes.

ratio of product flow to feed flow, is taken to be 0.1522, which is the value used by Rätz (1985) to produce 3% product and 0.3% tails from a feed of natural uranium.

In the first feed model, the feed gas is introduced as a radial flux of mass across the boundary at $x = x_T$. The flux is three radii in axial extent and centered about the axial midplane. The other boundary conditions are no tangential or vertical shear and no heat flux. Also, no source terms are used in this case. The results are given in Figs. 4a and 4b, and this model is designated as F1.

In the second feed model, designated F2, the source terms are used as given in Eq. (3.1). The mass is assumed to enter by the formula

$$M = M_0\delta(x - x^*)\, G(y) \tag{4.1}$$

where

$$G(y) = \begin{cases} 0 & 0 \le y < y^* - 1.5 \\ 1 & y^* - 1.5 \le y \le y^* + 1.5 \\ 0 & y^* + 1.5 < y \le y_T \end{cases} \tag{4.2}$$

where $y^* = y_T/2$ and δ is the Dirac delta function. This implies that the mass enters in a ring of axial extent equal to 3 radii centered about the midplane. For the source velocity $\mathbf{V} = (v_r, v_\theta, v_z)$, we choose $v_\theta = v_z = 0$ and $v_r = (\gamma RT_0)^{1/2}$, the sound speed for UF_6. This simulates the case of choked flow through the orifice in the center post. The streamlines and plots of e_F and m for this case are given in Figs. 5a and 5b. The third feed model, F3, is identical with F2 except that the azimuthal component of the source velocity is taken to be equal to the local velocity of solid body rotation. This assumes the feed flow has been spun up so that $v_\theta = \Omega r^*$. The same quantities are presented for this model in Figs. 6a and 6b.

The differences in the streamline plots for these three feed cases are subtle and do not provide as much information as the plots of the separation parameters. The three cases have quite different distributions of flow profile efficiency. Both the F1 and F2 cases have similar trends, with e_F being lower in the enricher section of the centrifuge than in the stripper section. However, the F3 case shows that e_F goes practically to zero below the feed position. In all three cases, m has a bimodal distribution, with the peak being in the stripper. The amplitudes of these curves are quite different, with the largest value being associated with F2 which models the feed gas introduced with no angular velocity.

It is interesting to compare these results with those distributions of e_F and m for the thermal drive and scoop drive cases. However, one cannot really infer what these parameters' distributions will be for combined

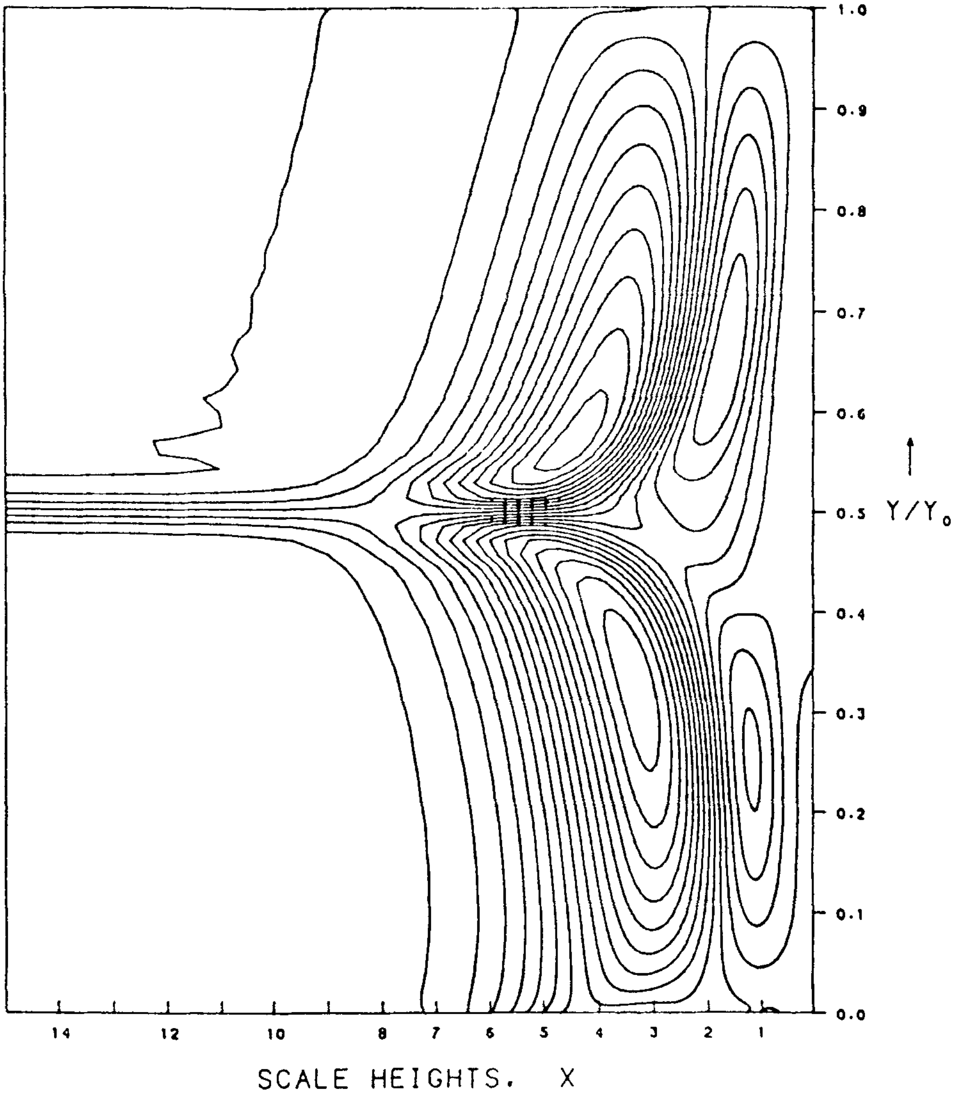

FIG. 4a Streamlines for feed drive with model F1, cut = 0.1522.

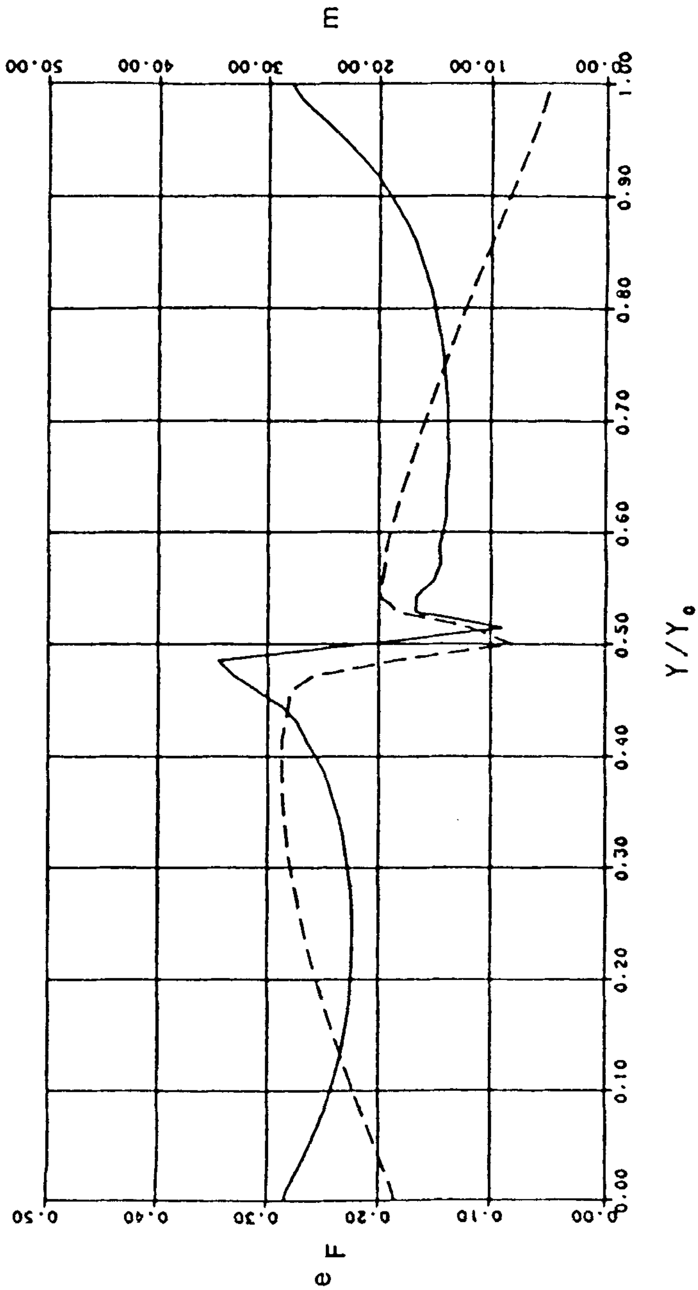

FIG. 4b Separation parameters e_F (——) and m (- -) versus axial position for feed model F1 with a feed rate of 1 kg/s.

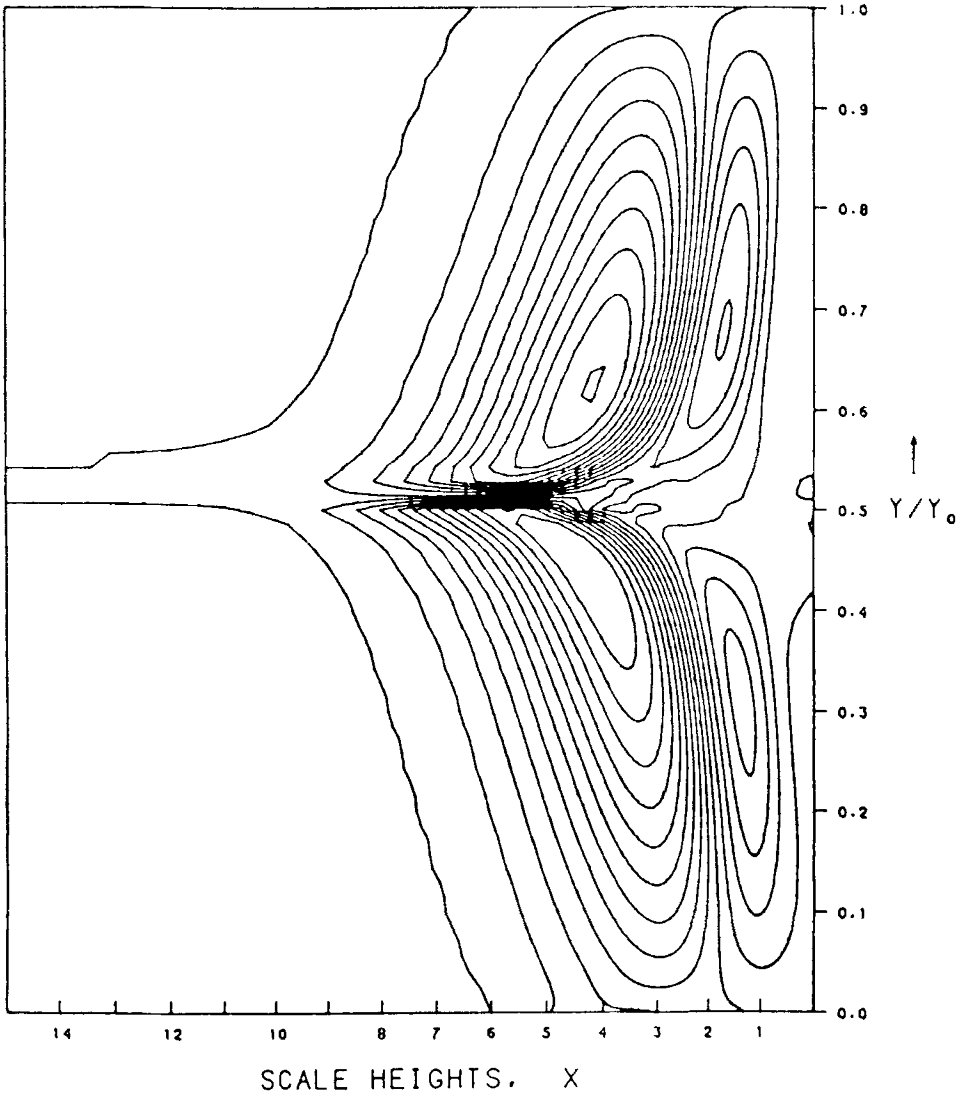

FIG. 5a Streamlines for feed drive with model F2, cut = 0.1522.

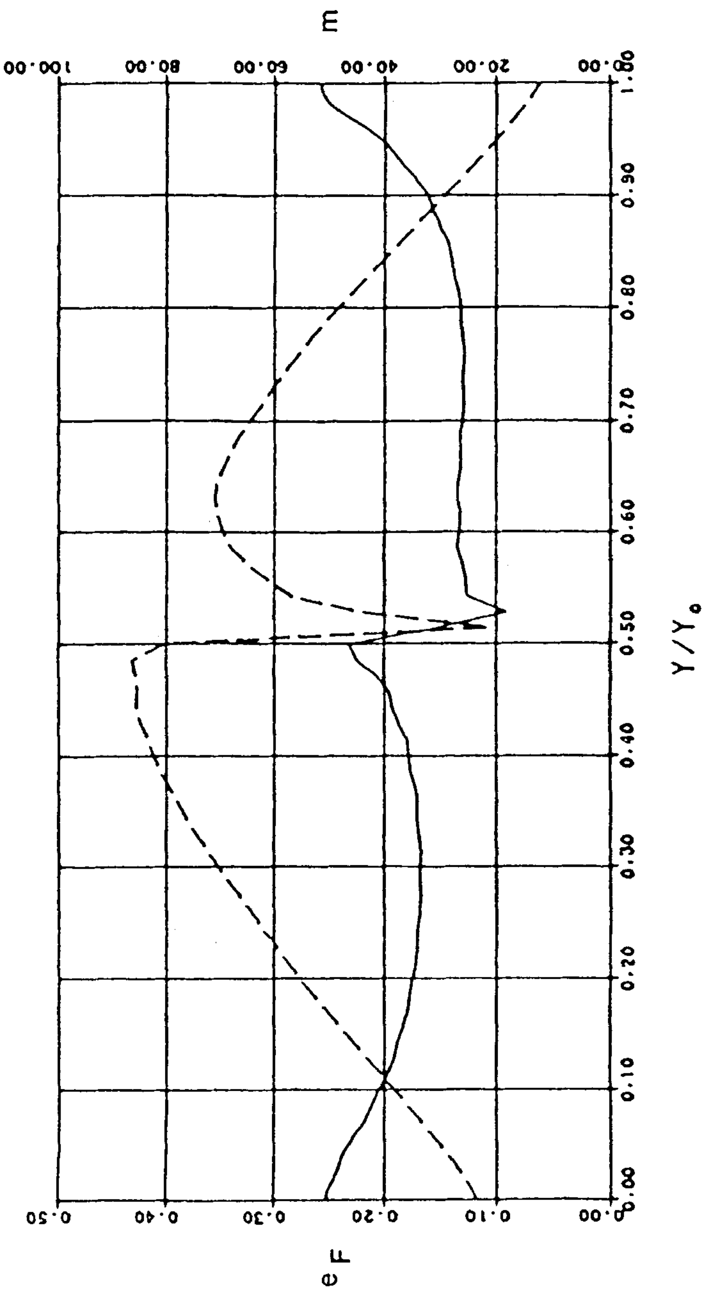

FIG. 5b Separation parameters e_F (——) and m (- -) versus axial position for feed model F2 with a feed rate of 1 kg/s.

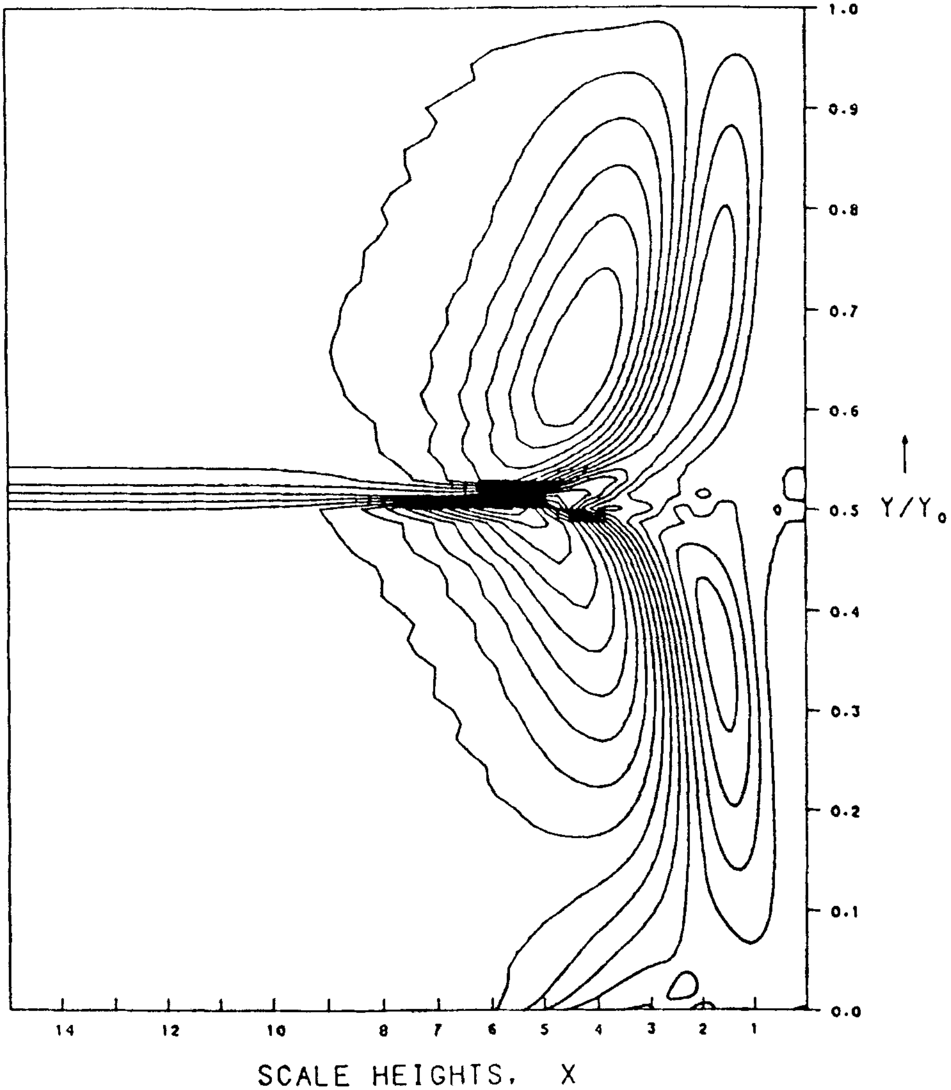

FIG. 6a Streamlines for feed drive with model F3, cut = 0.1522.

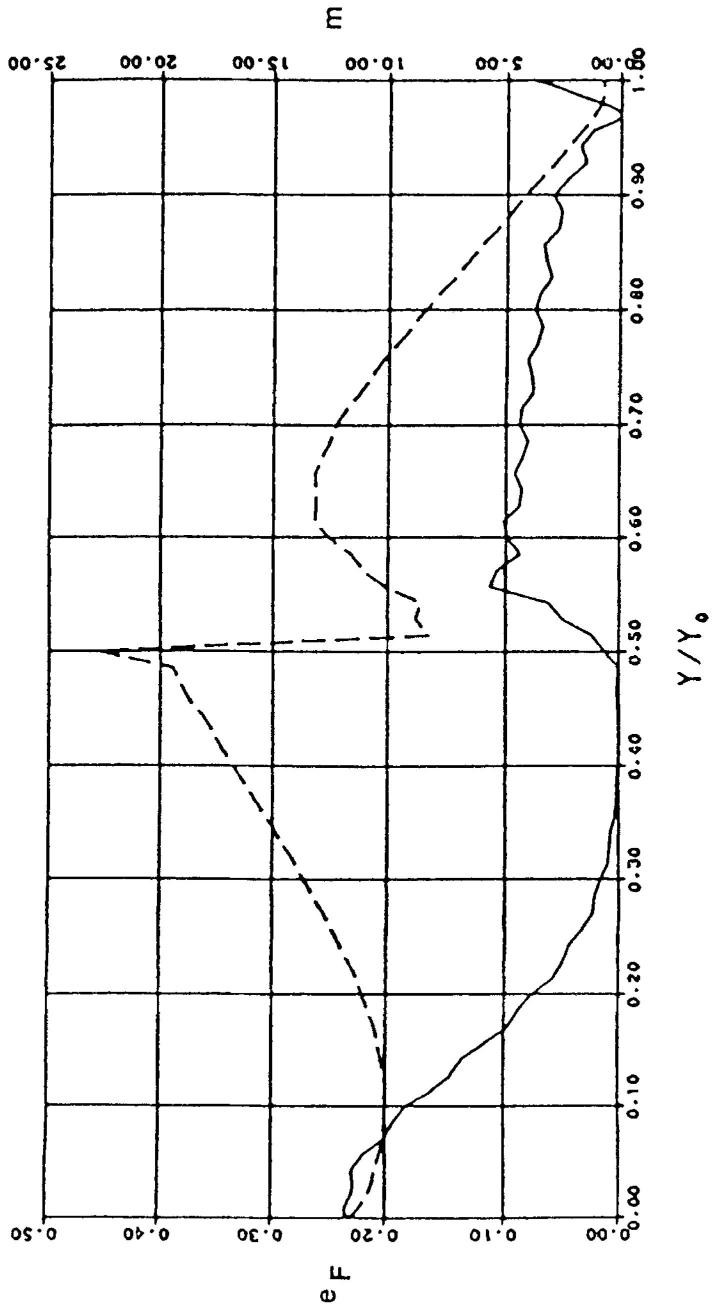

FIG. 6b Separation parameters e_F (——) and m (- -) versus axial position for feed model F3 with a feed rate of 1 kg/s.

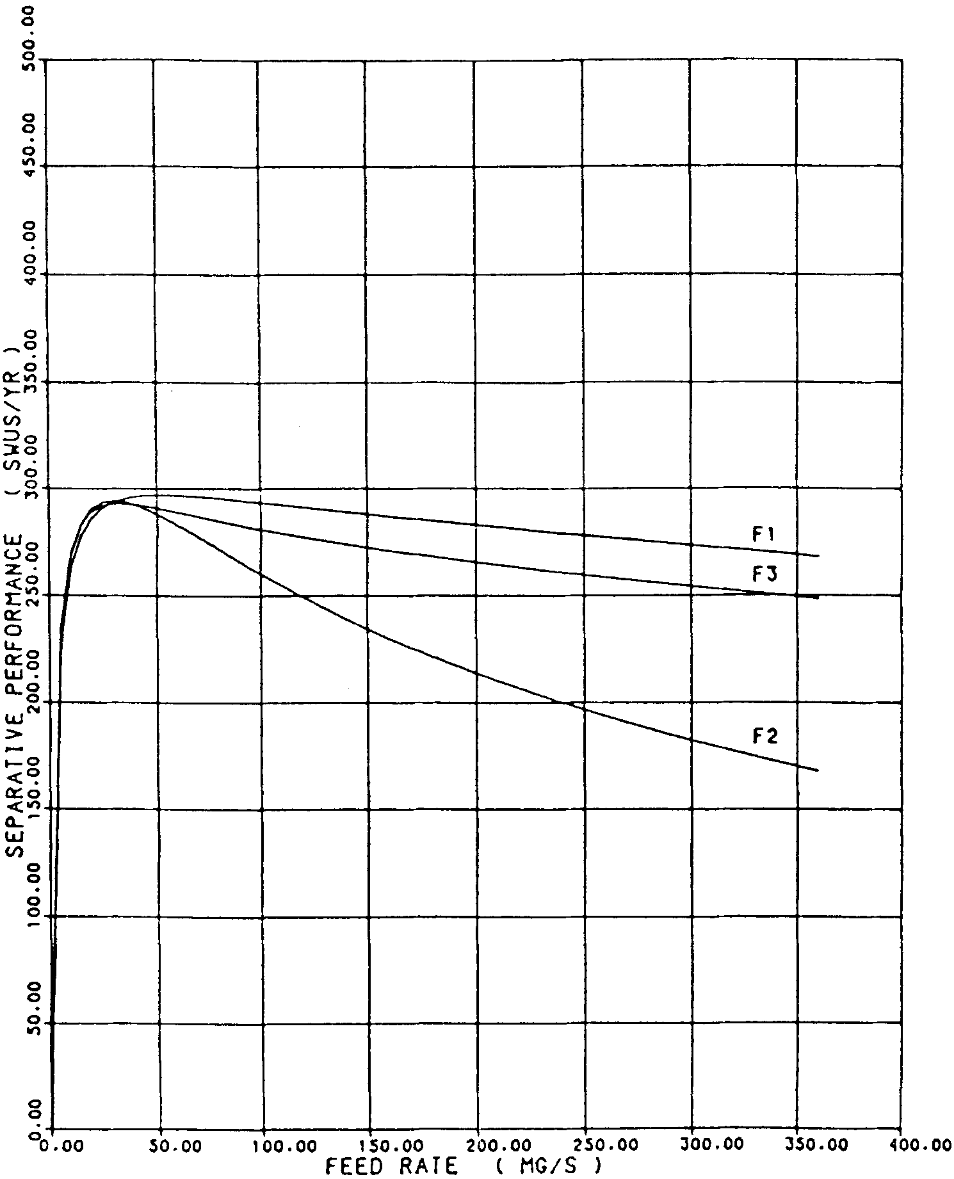

FIG. 7 Separative performance versus feed rate for centrifuge parameters in Table 1 and for each of the three feed models. The cut is fixed at 0.1522, and the separative performance at each point is optimized with respect to wall temperature gradient and scoop drag.

cases of feed drive, thermal drive, and scoop drive. Even though the fluid dynamic solutions may be combined in a linear fashion, e_F and m depend on the fluid dynamics in a nonlinear manner.

The separative performance was calculated using the Cohen–Onsager model of the transport equation which has been described by Hoglund et al. (11) and Von Halle (12). Figure 7 shows the separative work versus feed rate for each of these three feed models. These curves have been generated by keeping the cut fixed at 0.1522 and finding the optimal values of the wall temperature gradient and the scoop drag for each value of the feed rate. It is interesting that each of these models produces similar values for optimum separative performance at about the same feed rate. These results are tabulated in Table 2, and the corresponding fluid dynamic solutions are given in Figs. 8–10. The distributions e_F and m are different in all three cases, but the separative performance is practically the same.

Rätz [6] discussed how the separative performance of a centrifuge drops off as the feed rate is increased through its optimal value. He attributed this phenomenon to the fact that energy must be expended to accelerate the feed gas to the rotational velocity of the surrounding gas. The results presented in Fig. 7 support Rätz's hypothesis. Model F2 requires the acceleration of the feed gas and tends to show drastically decreasing performance compared to the other models as more feed is required to be spun-up. In model F3 the gas exits the center post already spun-up and apparently does less harm on the surrounding gas. Model F1 assumes neither tangential nor vertical shear is done by the feed gas and is therefore more similar to model F3.

A numerical study of one-stage enrichment was also performed in order to compare the results of this model with those of Rätz (6). The separative work was calculated as a function of feed rate with fixed cut and optimal values for scoop drag and wall temperature gradient, with the axial position of the feed as a parameter. For all three feed models, the optimal location was found to be approximately the axial midplane. Then, using feed model F1 with feed introduced at the midplane, the optimum separative performance versus feed rate was calculated using the values in Table

TABLE 2

Optimal values	F1	F2	F3
Feed rate (mg/s)	52.3	29.2	32.7
Separative performance (kg U/yr)	296.9	294.4	293.0
Scoop drag (dynes)	4948	3787	3640
Temperature gradient (K)	1.89	1.51	1.50

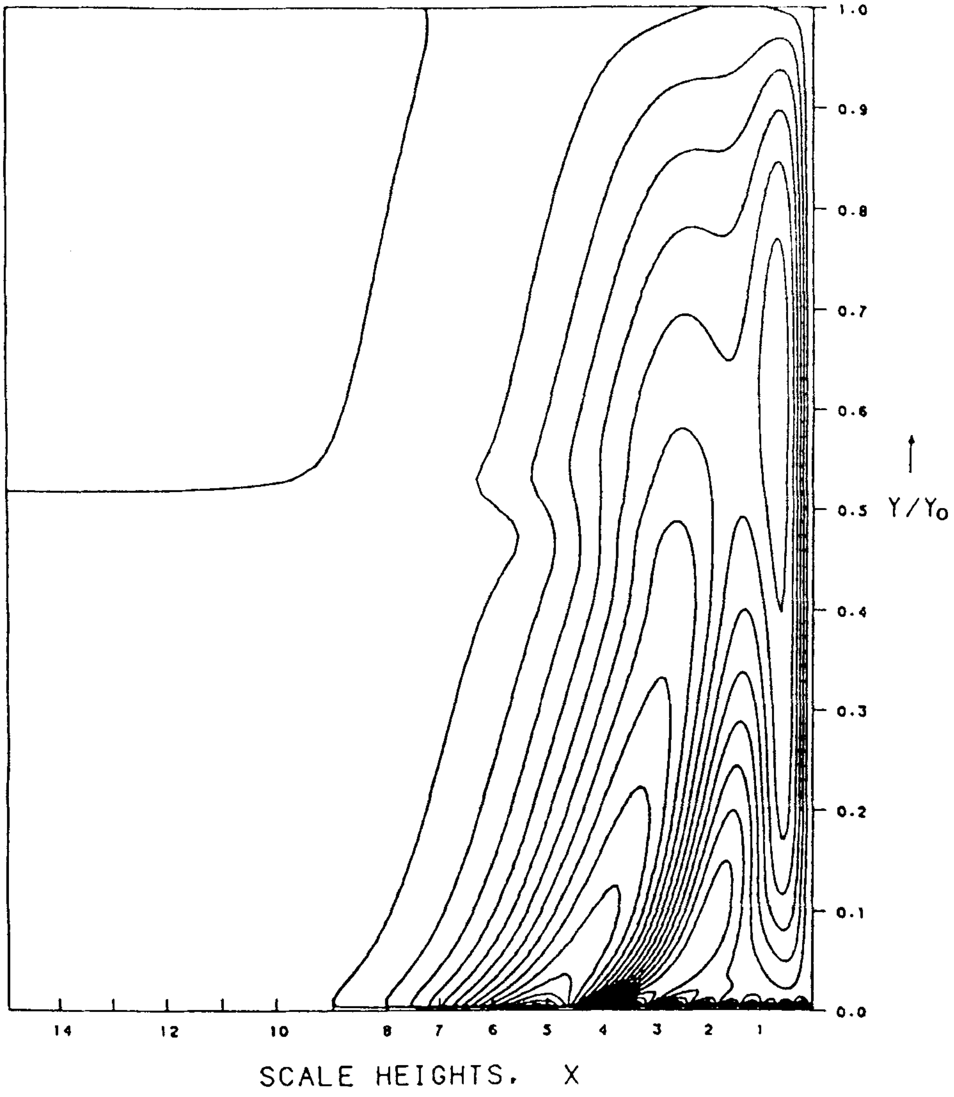

FIG. 8a Streamlines for optimal conditions described in Table 2 for feed model F1.

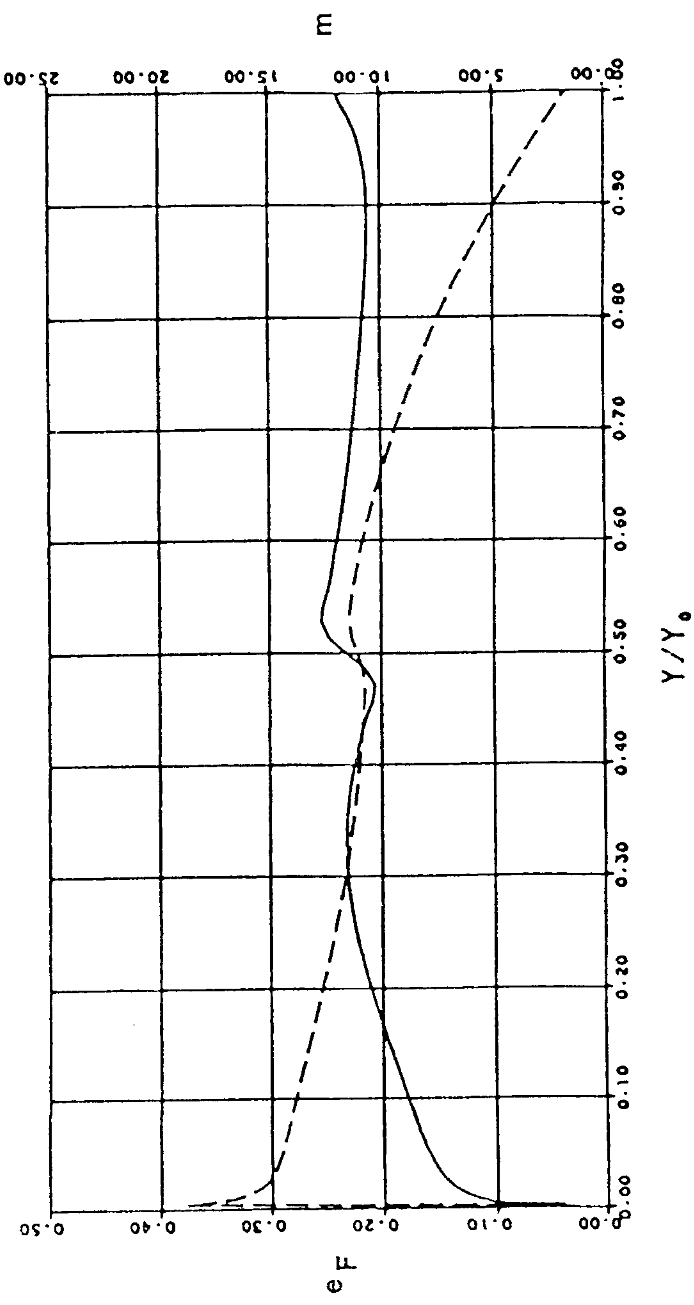

FIG. 8b Separation parameters e_F (——) and m (- -) versus axial position for optimal conditions with feed model F1.

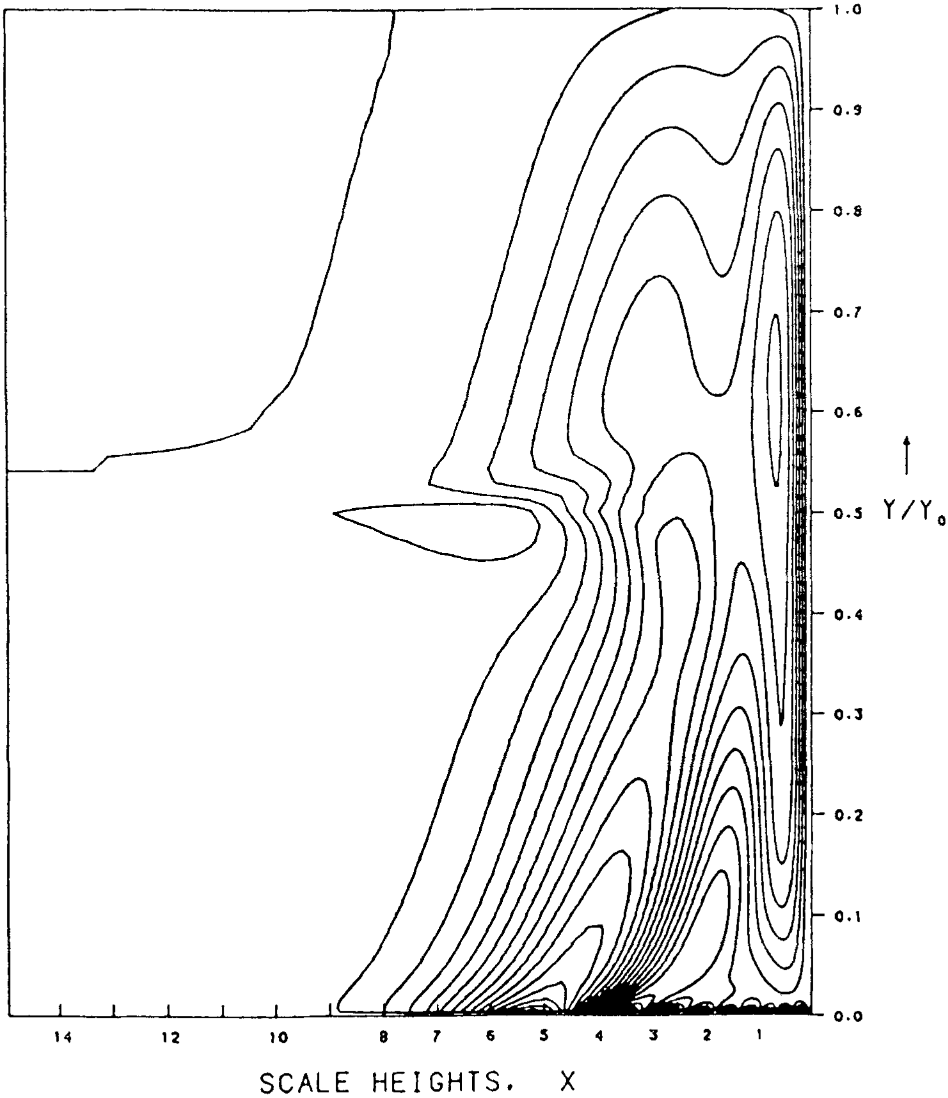

FIG. 9a Streamlines for optimal conditions described in Table 2 for feed model F2.

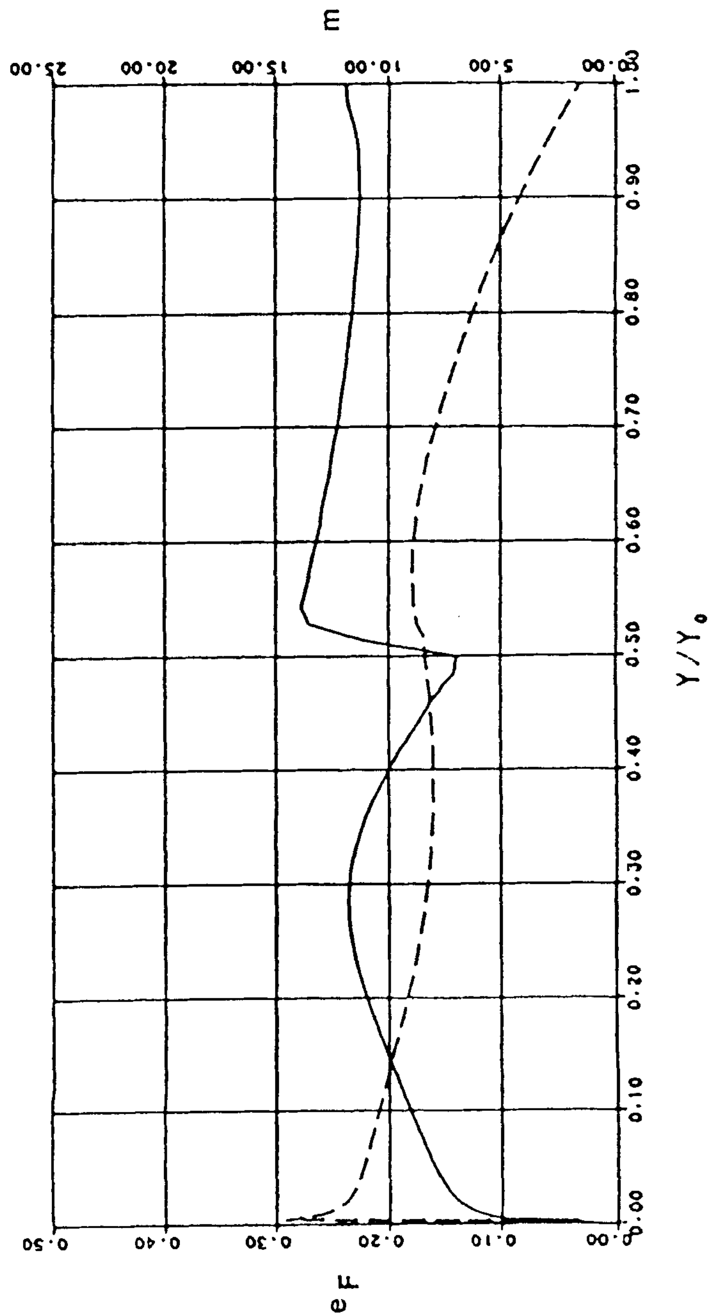

FIG. 9b Separation parameters e_F (——) and m (- -) versus axial position for optimal conditions with feed model F2.

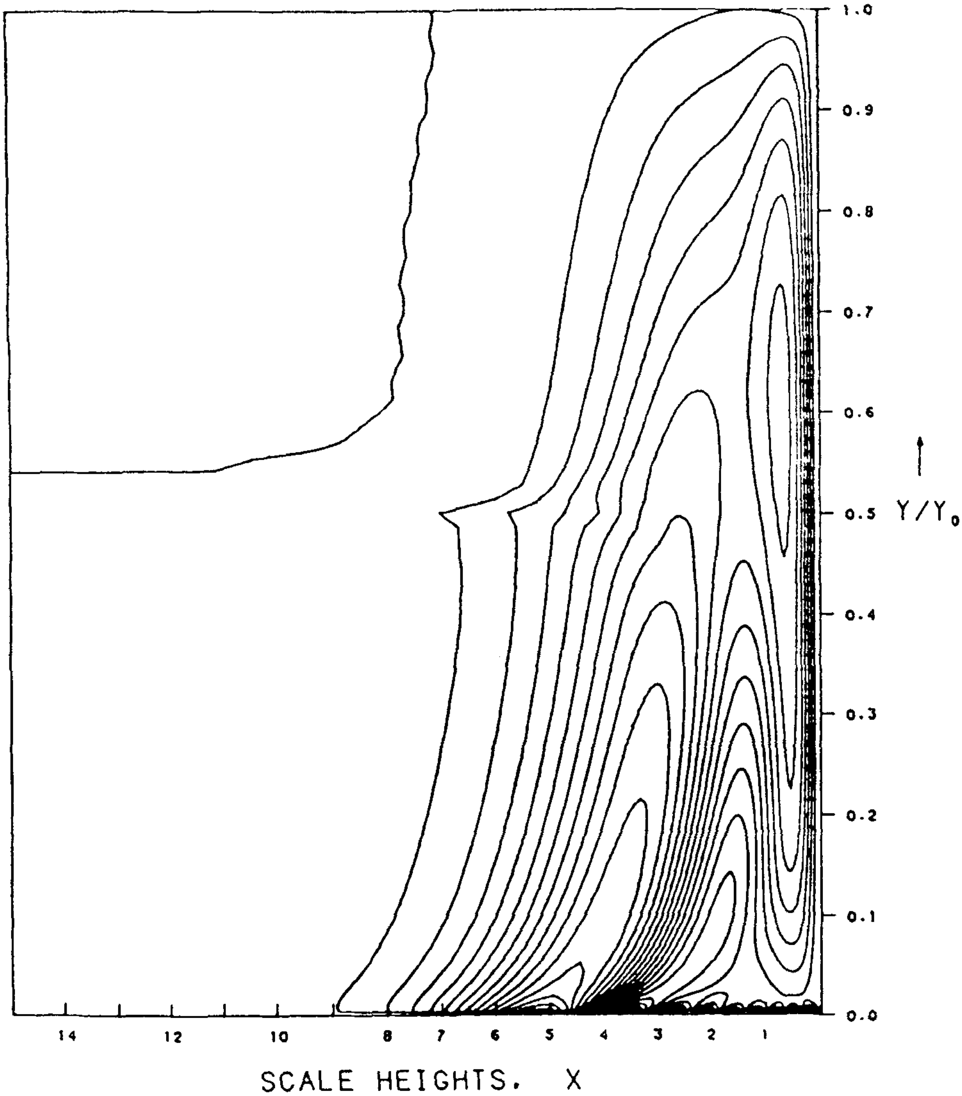

FIG. 10a Streamlines for optimal conditions described in Table 2 for feed model F3.

1 and peripheral speeds of 600, 800, and 1000 m/s. The results are given in Fig. 11. The locus of the points at which the product stream has a ^{235}U concentration of 3% is indicated by the straight line, and these results compare very well with those of Rätz (6). The loss in separative perfor-

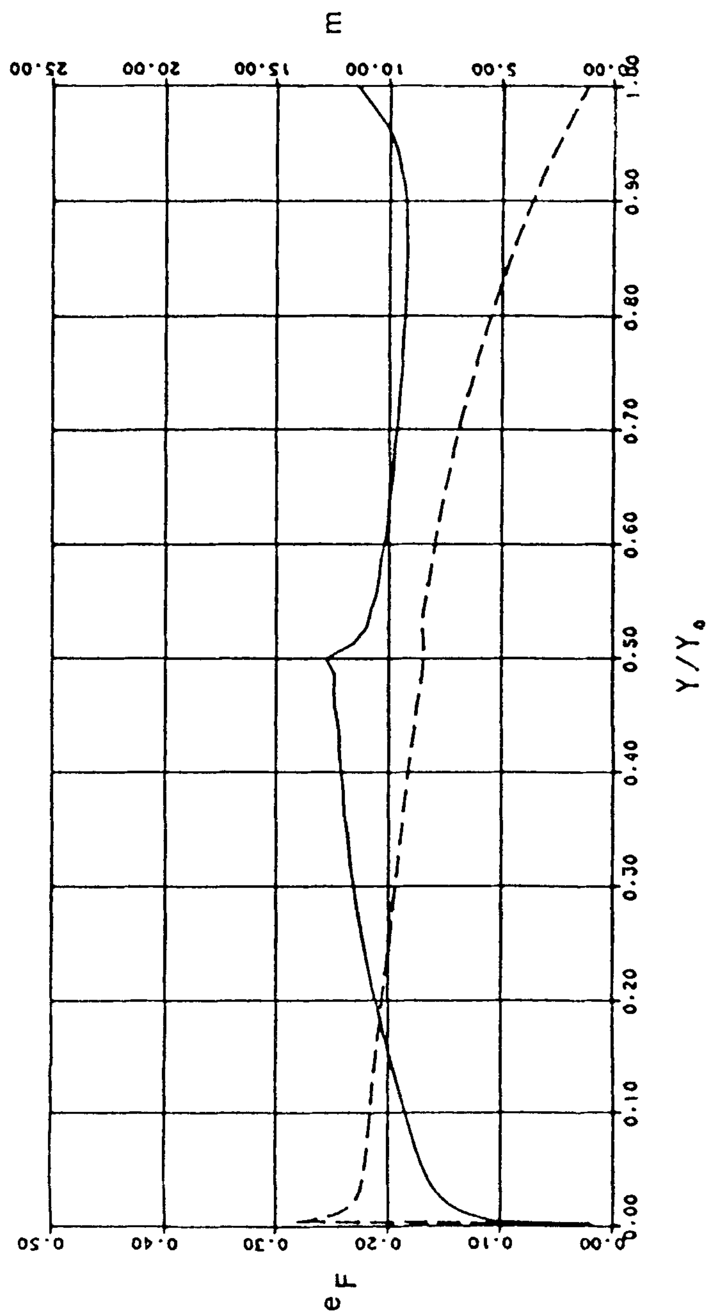

FIG. 10b Separation parameters e_F (——) and m (- -) versus axial position for optimal conditions with feed model F3.

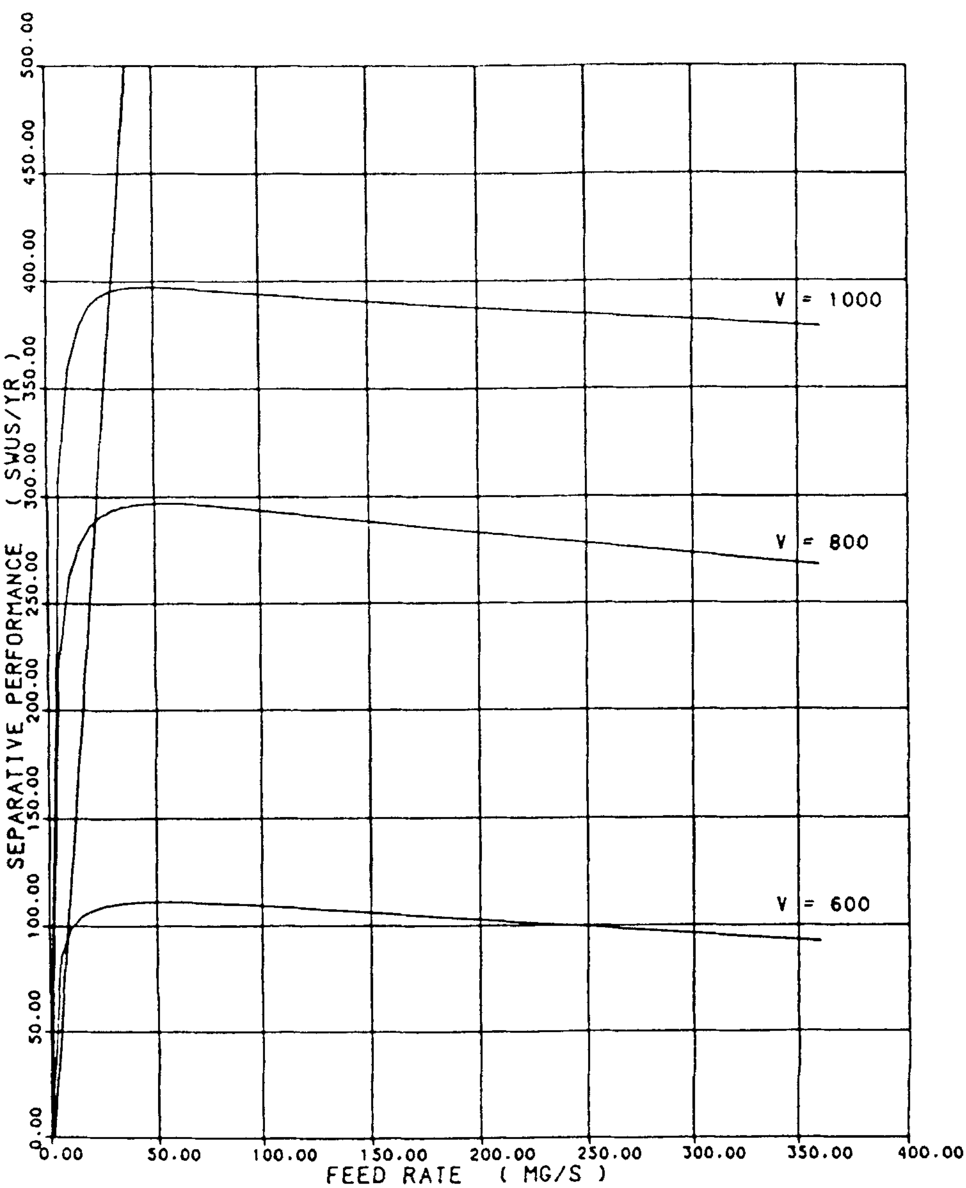

FIG. 11 Separative performance versus feed rate for centrifuge parameters in Table 1 plus peripheral speeds of 600 and 1000 m/s. These calculations are with feed model F1 and cut = 0.1522. The separative performance at each point is optimized with respect to wall temperature gradient and scoop drag. The line is the locus of points with product concentration 3% ^{235}U.

mance by operating at the 3% point is seen to be less as the peripheral speed is increased.

5. CONCLUSIONS

In summary, we have shown that the countercurrent flow induced by the introduction of feed gas is important in centrifuge design considerations. Also, the theory indicates the method of feed introduction can have an effect on the performance of the centrifuge. We have also indicated quite satisfactory agreement with the results predicted by Rätz using his more approximate model. This certainly shows the value of the computationally simpler model for getting the correct range of centrifuge operating parameters. Finally, both this study and that of Rätz indicate that one-stage enrichment is a reasonable objective using modern gas centrifuges.

REFERENCES

1. W. L. Roberts, "Gas Centrifugation of Research Isotopes," *Nuc. Instrum. Methods Phys. Res.*, *A282*, 271–276 (1989).
2. A. J. Szady, "Enrichment of Chromium Isotopes by Gas Centrifugation," *Ibid.*, *A282*, 277–280 (1989).
3. C. Ying and Z. Guo, "Some Characteristics for Multicomponent Isotope Separation," in *Proceedings of the Fourth Workshop on Separation Phenomena in Liquids and Gases* (C. Ying, Ed.), In Press.
4. V. D. Borisevich, G. A. Potapov, G. A. Sulaberidze, and V. A. Chuzhinov, "Multicomponent Isotope Separation in Cascades with Additional External Flows," *Ibid.*
5. V. E. Fillippov and Lu. Y. Sosnin, "Modelling of Gas Flow and Separation Process of Multicomponent Mixture of Isotopes in Countercurrent Centrifuge with Internal Input of Feed," *Ibid.*
6. E. Rätz, "One-Stage Enrichment with Centrifuges," in *Proceedings of the Sixth Workshop on Gases in Strong Rotation* (Y. Takashima, Ed.), 1985, pp. 621–654.
7. H. G. Wood and J. B. Morton, "Onsager Pancake Approximation for the Fluid Dynamics of a Gas Centrifuge," *J. Fluid Mech. 101*, 1–31 (1980).
8. H. G. Wood and G. Sanders, "Rotating Compressible Flows with Internal Sources and Sinks, *Ibid.*, *127*, 299–313 (1983).
9. H. G. Wood and R. Babarsky, "Analysis of a Rapidly Rotating Gas in a Pie-Shaped Cylinder," *Ibid.*, *239*, 249–271 (1992).
10. G. R. Cooper and J. B. Morton, "Driven Wave Motions in a Rotating Gas," *J. Fluids Struct.*, *2*, 453–477 (1988).
11. R. L. Hoglund, J. Shacter, and E. Von Halle, "Diffusion Separation Methods," in *Encyclopedia of Chemical Technology*, Vol. 7, 3rd ed. (R. E. Kirk and D. F. Othmer, Eds.), Wiley, New York, 1979.
12. E. Von Halle, "The Countercurrent Gas Centrifuge for the Enrichment of U-235, in *Proceedings 70th Annual Meeting AIChE*, New York, 1977.

Received by editor November 14, 1994